

Power Aggregation from Multiple Energy Harvesting Devices via a Conductive Embroidered Cloth

Yuuichi Masuda, Akihito Noda, and Hiroyuki Shinoda

Abstract— This paper proposes a power aggregation scheme using small energy harvesting (EH) devices distributed on a special cloth embroidered with conductive threads. Each EH device is removable, like a pin badge, by using a special connector consisting of a tack and a clutch, without one-to-one wiring. In a conventional EH system, each device, such as a sensor node, has its own individual EH element. Power aggregation systems using a wide variety of EH devices can supply more power than conventional EH systems, to a power-intensive device. The aggregation efficiency with respect to the number of connected devices and the variation in the output of each device are demonstrated by circuit simulation. The experimental results demonstrate the feasibility of power aggregation circuits.

I. INTRODUCTION

Energy Harvesting (EH) is a promising technology for wearable and Internet-of-Things (IoT) devices [1] [2] [3]. One power generation element in one device is common in conventional EH systems, while the use of multiple elements is rare [4]. While the sensor chip shown in Fig. 1 can be driven by one power generation element (PGE), the host device that collects data frequently from sensors cannot be, because it consumes significantly more power than one sensor chip. The energy generated in a small area/volume of the host device from its surrounding environment is insufficient to drive it. However, the host device may be driven by the entire body's energy, collected from multiple PGEs distributed across the clothing. However, the wiring to each PGE raises an implementation problem.

In this paper, we propose a power aggregation scheme from multiple PGEs to the storage terminal without one-to-one wiring by using conductive-thread-embroidered fabric (CTEF) and tack-type connector [5] [6]. Penetration fixing and contact conduction are simultaneously realized at arbitrary positions on the CTEF, as shown in Fig. 1. Following are the advantages of our proposal: 1) the amount of power generation can be increased with the number of PGEs, 2) each PGE can be placed at an arbitrary position, and 3) a multi-source EH system can be realized.

This work was supported in part by the JST ACCEL Embodied Media Project (Grant Number JPMJAC1404) and JSPS KAKENHI Grant Number 17H04685.

Y. Masuda and H. Shinoda are with the Department of Complexity Science and Engineering, The University of Tokyo, 5-1-5 Kashiwanoha, Kashiwa-shi, Chiba, Japan (e-mail: masuda@hapis.k.u-tokyo.ac.jp; hiroyuki_shinoda@k.u-tokyo.ac.jp).

A. Noda is with the Department of Mechatronics, Nanzan University, 18 Yamazato-cho, Showa-ku, Nagoya-shi, Aichi, Japan (e-mail: anoda@nanzan-u.ac.jp).

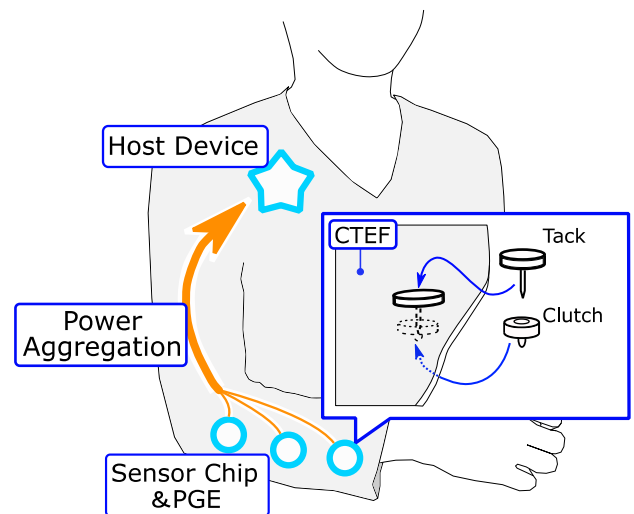


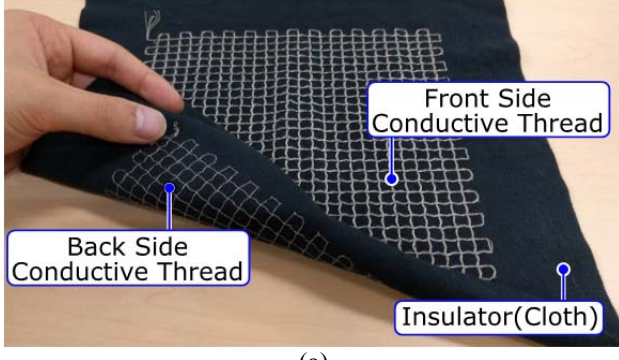
Fig. 1 Concept of power aggregation system by using wearable two-dimensional communication sheet and tack connector.

In this scheme, the number of PGEs can be adjusted according to the required amount of electricity by simply attaching more PGEs. Free arrangement allows practical installation, such as using PGEs as buttons. Multi-source EH systems increase the types of available energy sources. Moreover, the diversity of EH sources will decrease the fluctuation of generated power due to any changes in environmental conditions.

When PGEs with different output voltages are directly connected in parallel, the output current of the high-voltage PGE flows not only to the storage terminal, but also to the low-voltage PGE, leading to energy loss.

For example, assuming that one of the two solar cells connected in parallel is under shade, which causes the output to lower drastically, the solar cell under shade functions as a diode [7] [8]. Most of the output current of the other solar cell flows to the ground via the solar cell under shade. In other words, reverse current prevention is necessary for efficient power aggregation.

This paper presents a circuit configuration that efficiently collects the output from the PGEs connected in parallel via the CTEF to the storage terminal. In the next section, the structure of the CTEF and tack-type connector is described. In Section III, the circuit configuration and simulation results are demonstrated. The experimental verification is presented in Section IV. Finally, we will conclude this paper in Section V.



(a)

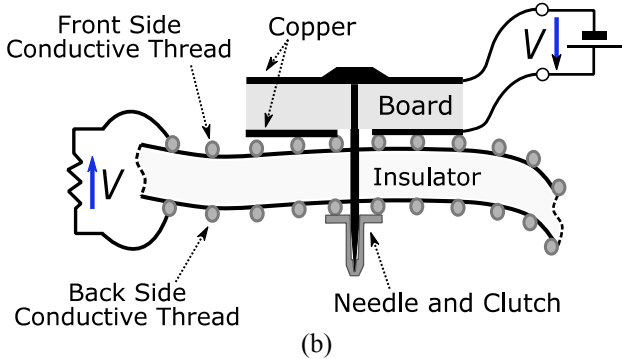


Fig. 2 (a) A conductive-thread-embroidered fabric. (b) Cross-sectional view when a tack connector is penetrated and fixed to a sheet.

II. CONDUCTIVE EMBODIES AND TACK CONNECTORS

Fig. 2 shows the structure of the CTEF and tack-type connector [5] [6]. The CTEF shown in Fig. 2 (a) is a transmission path, with a two-dimensional spread by sewing conductive threads on both sides of a cloth-like insulator. Fig. 2 (b) shows the cross-sectional view when a needle is pierced from the front side of the CTEF and fixed with a metallic clutch on the back side. In the tack-type connector, a metallic needle is fixed and conducted by soldering it to the surface of the double-sided copper clad board (the upper side of Fig. 2 (b)). The conductive threads on the front and back sides conduct with the backside of the board and the front side of the clutch when penetrating and fixing. If the backside conductive thread is grounded, the board surface can be designed as a ground.

It should be noted that the front-side conductive thread should not be in contact with the needle in order to prevent short circuit. The copper pattern on the bottom side of the board is also electrically isolated from the needle.

III. POWER AGGREGATION SYSTEM

In this section, we present a circuit diagram, which aggregates power from multiple PGEs via a CTEF. We also confirm its validity by circuit simulation. The aggregation efficiency is evaluated as the ratio of the charge speed of the storage terminal to the total power generation speed of each PGE. For example, when the total output of the PGEs is 100 mW, with the charging speed of the power storage terminal being 80 mW, the aggregation efficiency is 80%.

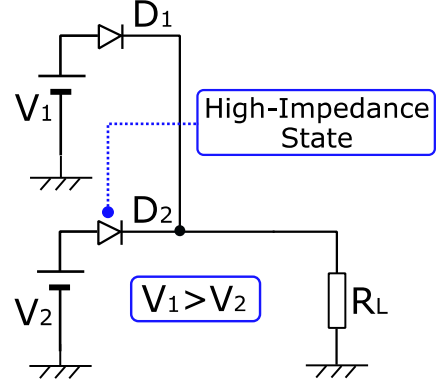


Fig. 3: Maximum value selection circuit.

As described in Section □, when the PGEs with different output voltages are directly connected in parallel, the current flows back to the element, decreasing the aggregation efficiency. The diode can stop the reverse current. However, it causes the following problems.

When the two voltage sources V_1, V_2 are connected in parallel to the load R_L via the diodes D_1, D_2 , this circuit becomes the maximum value selection circuit, as shown in Fig. 3. Assuming $V_1 > V_2$, D_2 experiences a high-impedance state due to the reverse bias, causing the electrical path from V_2 to R_L to break. Thus, even when a large number of PGEs are connected to the CTEF via diodes, only one maximum voltage PGE can be connected to the storage terminal.

The power aggregation circuit proposed in this paper is shown in Fig. 4. This circuit has the following two functions: 1) The output of each PGE is temporarily stored in the capacitor C_n ($n = 1, 2, \dots, N$); and 2) the temporarily stored energy is transferred to the super capacitor C_{OUT} . The first one is referred to as the temporary power storage function, while the other one is referred to as the power aggregation function.

In the temporary power storage function (the switch is

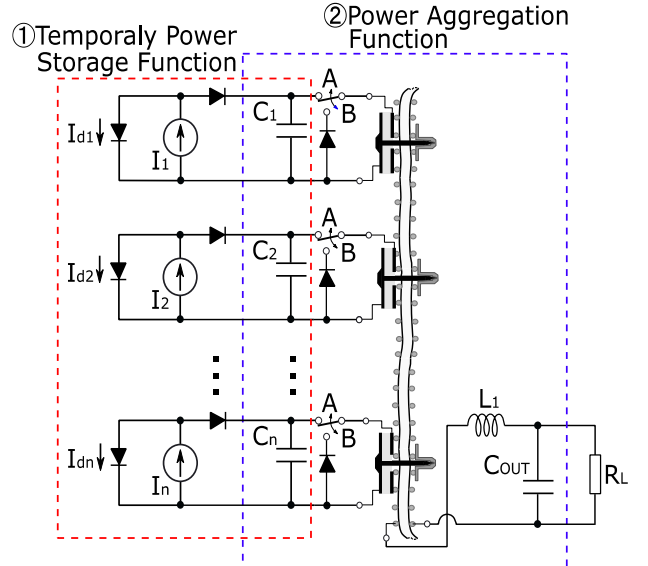


Fig. 4 Schematic diagram of power aggregation circuit.

turned to B side), each PGE is electrically disconnected from the CTEF. No current flows from other PGEs. In the current aggregation function (switch position A), energy moves from C_n to the coil L_1 . After the switch is moved to the B side again, energy flows from L_1 to C_{OUT} .

When capacitors (C_1, C_2) with different voltages are directly connected, some energy is lost by wire resistance through an impulsive current. This is apparent from the following equations.

$$U_{start} = \frac{Q_{1,start}^2}{2C_1}, \quad (1)$$

$$\begin{aligned} U_{end} &= \frac{Q_{1,end}^2}{2C_1} + \frac{Q_{2,end}^2}{2C_2} \\ &= \frac{1}{2C_1} \left(\frac{C_1 Q_{1,start}}{C_1 + C_2} \right)^2 + \frac{1}{2C_2} \left(\frac{C_2 Q_{1,start}}{C_1 + C_2} \right)^2 \quad (2) \\ &= \frac{Q_{1,start}^2}{2(C_1 + C_2)}, \end{aligned}$$

where U_{start} denotes the total energy of C_1 and C_2 when C_2 is empty. $Q_{1,start}$ denotes the charge of C_1 at that time. U_{end} denotes the total energy of C_1 and C_2 , when the voltage of both capacitors becomes constant. $Q_{1,end}$, $Q_{2,end}$ denote the charges of C_1, C_2 at that time. $U_{start} > U_{end}$ indicates the energy loss. If a coil and switch are used between capacitors, $U_{start} = U_{end}$ can be realized, unless switching losses are taken into account.

A. Circuit Simulations

In this subsection, we show the aggregation efficiency of the circuit shown in Fig. 4 by circuit simulation with LT SPICE [9]. The number of PGEs and the distribution of each PGE output are changed in the simulation. The PGE is assumed to be a commercially available small solar cell (Sphelar Power Corporation, KSP-F12-12S1P-W1-X [10]). The solar cell is modeled with a current source I_n , generated by light, and a diode current I_{dn} [7] [8]. $I_{out,n}$, which is the output current of the solar cell, is expressed as:

$$I_{out,n} = I_n - I_{dn}, \quad (3)$$

$$\text{where } I_{dn} = I_o \left\{ \exp \frac{qV_{out,n}}{nkT} - 1 \right\}, \quad (4)$$

where I_o is the reverse saturation current and n denotes the diode performance index. I_o and n depend on the type of solar cell. k is the Boltzmann constant, T is the absolute temperature, q is the elementary charge, and $V_{out,n}$ is the operating voltage.

The aggregation efficiency is the ratio of the charge speed of the storage terminal to the total power generation speed of each PGE. The charge speed is calculated using the capacity and the time derivative of the instantaneous voltage across C_{OUT} . The total power generation speed is calculated using the maximum solar cell output and the number of connected solar cells.

For the control of the switch, we assumed the use of commercially available energy harvest power supply IC

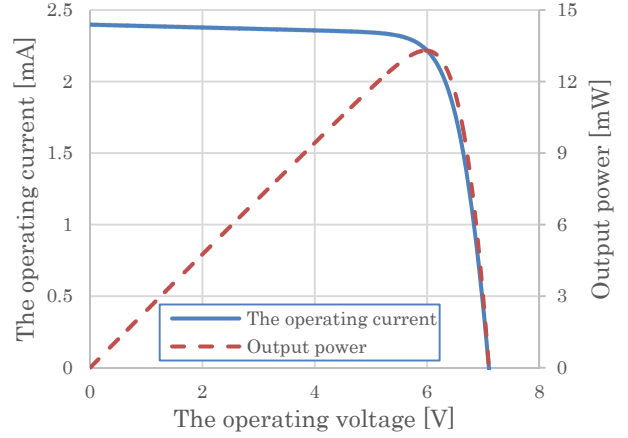


Fig. 5 I-V curve of solar cell simulation model.

(Linear Technology Corporation, LTC3588-1 [11]). The SPICE library, provided by Linear Technology, is used for modeling.

Other parameters used in the simulation are shown in Table

TABLE □. Circuit parameters in SPICE simulation

I_n	2.4 mA
I_o	$1 \cdot 10^{-13}$ A
n	11.5
C_n	47 μ F
L_1	10 μ H
C_{OUT}	4700 μ F
R_L	250 k Ω

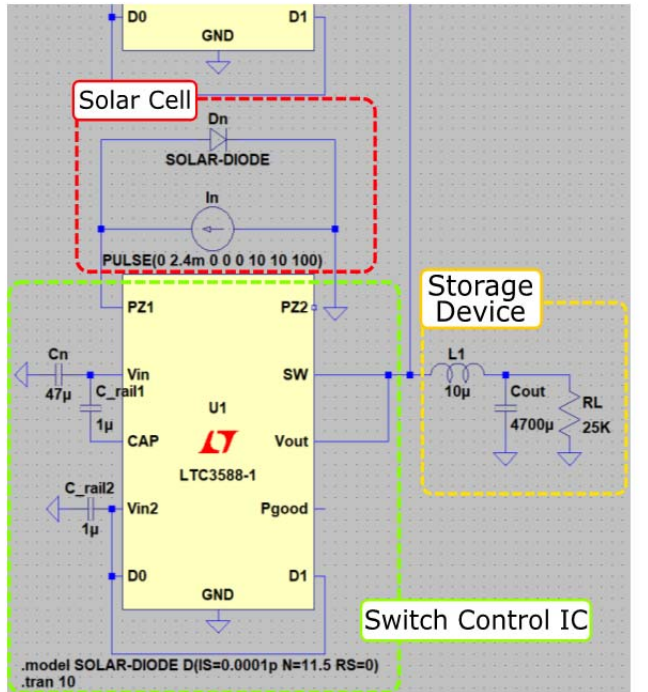


Fig. 6 SPICE simulation model.

1. The values of I_n , I_o and n were determined with reference to the assumed solar cell data sheet [10]. The I-V curve of the solar cell model with the parameters in Table 1 is shown in Fig. 5. The operating current, at an operating voltage of 6 V, is 2.21 mA. The maximum output is 13.3 mW. This value is used in calculating the total power generation speed.

The SPICE simulation model is shown in Fig. 6. The simulation results of the aggregation efficiency for each number of solar cells are shown in Fig. 7. When the number of solar cells is one, the charging speed is 8.3 mW, which is 62.5% of the maximum output of the solar cell. The switching loss and the operating voltage of the solar cell are believed to be the cause of efficiency reduction. The operating voltage is in the range of 3.9–5.1 V, while the maximum output is obtained at 6 V.

When the number of connected devices increases from 1 to 10, the aggregation efficiency increases from 62.5% to 67.5%. Efficiency is not reduced by increasing the number of devices in this system. Instead, it is advantageous to use several terminals. However, the timing of switching at each device is synchronized in this simulation.

The aggregation efficiency for each dispersion value of output current is shown in Fig. 8. The number of connected

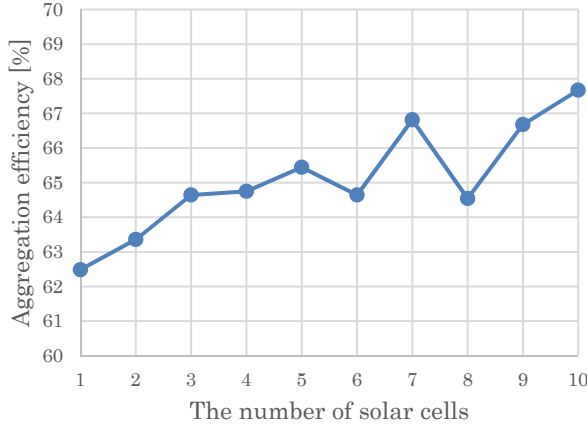


Fig. 7 Aggregation efficiency for each number of solar cells.

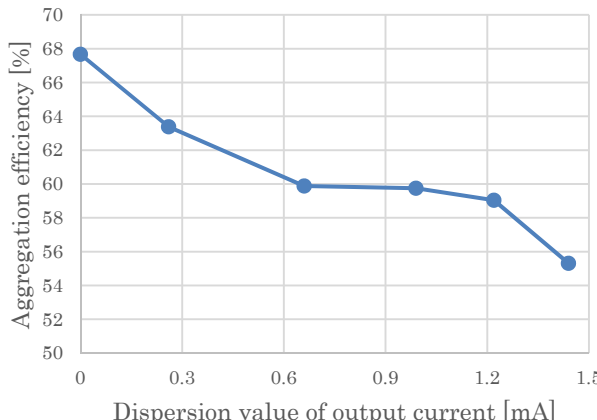


Fig. 8 Aggregation efficiency for each dispersion value of output current.

devices is fixed at 10. The dispersion is adjusted by changing I_n between 0 and 2.4 mA. When the dispersion increases from 0 mA to 1.45 mA, the aggregation efficiency decreases by 12.3%.

The efficiency is reduced by directly connecting capacitors (C_n) with different voltages via the CTEF. As shown by (1) and (2), energy loss occurs when capacitors with different voltages are directly connected. Since the power generation speed of each PGE is different, the switching timing varies depending on the device. Thus, the opportunity to directly connect the capacitors with different voltages increases.

IV. EXPERIMENT

In this section, we measure and evaluate the charging speed and aggregation efficiency based on the number of devices, by using the prototype EH device. The measurement setup is

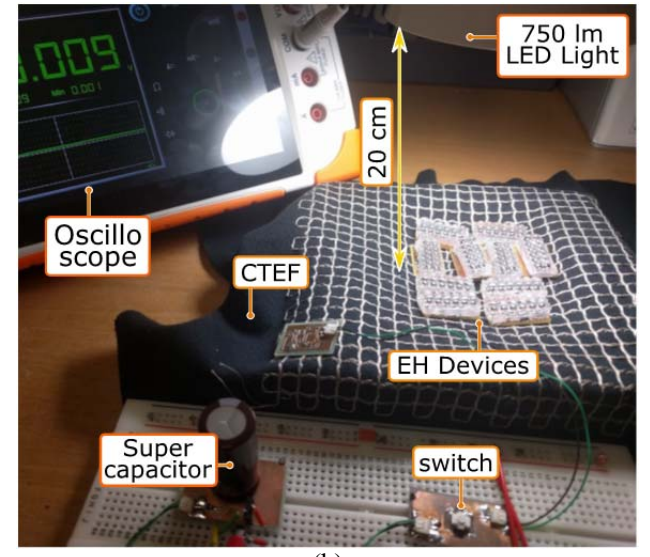
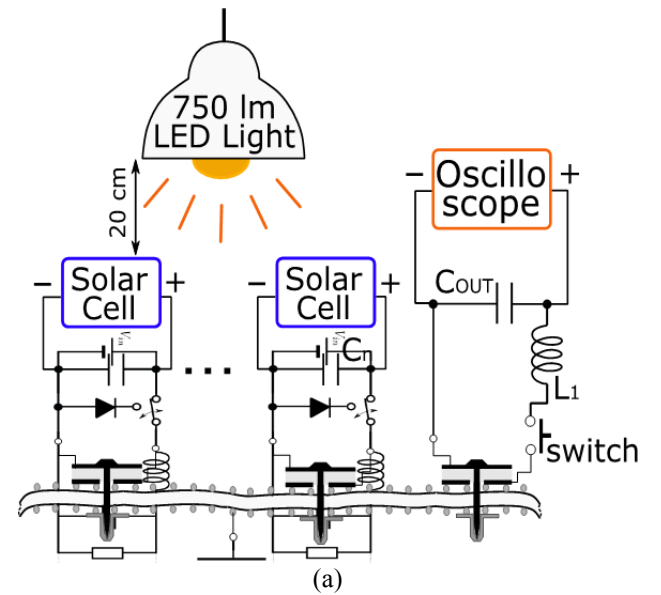


Fig. 9 (a) Schematic diagram of measurement setup. (b) Photo of the setup.

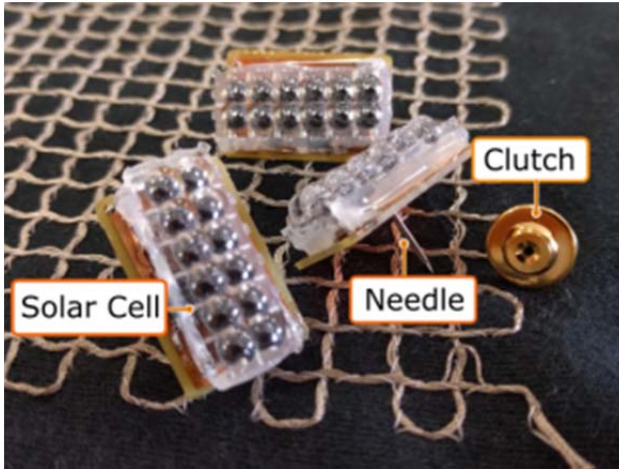


Fig. 10 Photo of the prototype EH device.

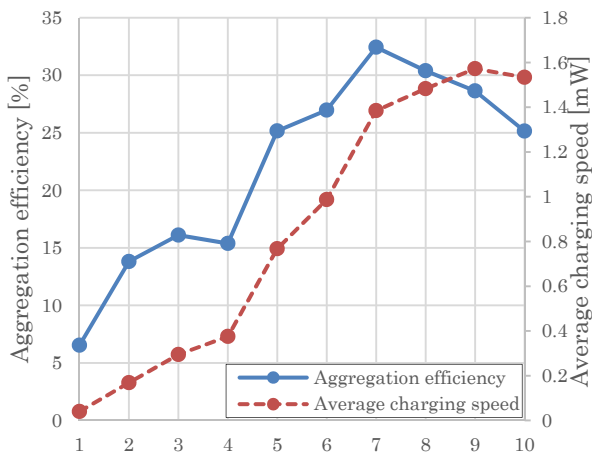


Fig. 11 Aggregation efficiency and average charging speed for the number of EH devices.

shown in Fig. 9. The prototype EH device is composed of a tack-type connector, a solar cell, and a switch control IC, as shown in Fig. 10.

Each EH device is connected to the CTEF with a tack-type connector. The oscilloscope measures the voltage of the super capacitor every 100 ms. When the switch is pushed, the super capacitor begins to charge. Voltages at five points from the start of charge time to the end time are measured.

The average of the charge speed thus obtained is shown in Fig. 11. The aggregation efficiency is also plotted, which is calculated from the average charge speed and the total output power of solar cells. An LED light source of 750 lumens is installed at about 20 cm above the solar cell. The output power of the solar cell varies between 0.6 and 0.7 mW, depending on the position.

The aggregation efficiency begins to show a downward trend when the number of EH devices is 7. As in the simulation result shown in Fig. 8, variation in the switching time of the EH devices reduces the efficiency. The charging speed peaks when the number of EH devices is 9. In order to use a larger

number of EH devices and increase the charging speed, the energy loss indicated by (1) and (2) should be prevented. The use of diodes or the synchronization of the switching time at each EH device is an effective solution.

V. CONCLUSION

We proposed a power aggregation scheme from multiple EH devices to a power storage device without one-to-one wiring by using a tack-type connector and a fabric sheet embroidered with conductive threads. Efficient aggregation cannot be realized by directly connecting all PGEs to CTEF, because the output current of the PGE with the highest output voltage is consumed in part by other PGEs generating lower voltages. The proposed circuit solved the above-mentioned problem using the temporary power storage function and the power aggregation function.

The simulation results show that the aggregation efficiency increases as the number of connected EH devices increases when the switching time of all the devices is synchronized. It also shows that switching time mismatch of all the EH devices decreases the efficiency. The mismatch increases the opportunity for directly connecting capacitors with different voltages via the CTEF, which results in energy loss.

The experimental result shows that efficiency shows a downward trend when the number of connected EH devices is 7 for the above reasons.

ACKNOWLEDGMENT

We thank Mr. Yoshiaki Hirano and Ms. Junko Yamada, Teijin Limited, for providing the CTEF materials.

REFERENCES

- [1] M. Ku, W. Li, Y. Chen, S. Member, and K. J. R. Liu, "Advances in Energy Harvesting Communications : Past , Present , and Future Challenges," *IEEE Trans. Communications Surveys & Tutorials*, vol. 18, no. 2, pp. 1384–1412, 2016.
- [2] M. Magno and D. Boyle, "Wearable Energy Harvesting: From Body to Battery," in *Proc. IEEE 2017 12th International Conference on Design & Technology of Integrated Systems In Nanoscale Era (DTIS)*, 2017, pp. 1–6.
- [3] P. Spies, M. Pollak, L. Mateu, "Handbook of Energy Harvesting Power Supplies and Applications," Florida: CRC Press, 2015, pp. 505–563.
- [4] A. S. Weddell, M. Magno, G. V Merrett, D. Brunelli, B. M. Al-hashimi, and L. Benini, "A Survey of Multi-Source Energy Harvesting Systems," in *Proc. IEEE Design, Automation & Test in Europe Conference & Exhibition (DATE) 2013*, 2013, pp. 905–908.
- [5] A. Noda, Y. Tajima and H. Shinoda, "Multiplex Wireless Power Transfer to Actuators Distributed on Flexible 2-D Communication Sheet for Wearable Tactile Display," in *Proc. the 17th SICE System Integration Division Annual Conference*, 2016, pp. 1349–1353. (in Japanese)
- [6] A. Noda and H. Shinoda, "Frequency-Division-Multiplexed Signal and Power Transfer for Wearable Devices Networked via Conductive Embroideries on a Cloth," in *2017 IEEE MTT-S International Microwave Symposium*, 2017, pp. 1–4.
- [7] T. Kunihiro, S. Etsuo, Y. Ejii, "Simulated Power Source Based on Output Characteristics of Solar Cell," *IEEJ Trans. Industry Applications*, vol. 113, no. 6, pp. 753–759, 1993.
- [8] Y. Kuwano, S. Nakano, Y. Kishi, M. Onishi, "Solar cells and their applications," Tokyo: Power, 1994, pp. 11–14.
- [9] Linear Technology. LTspice. [Online] Available: <http://www.linear-tech.co.jp/designtools/software/#LTspice>

- [10] Sphelar Power. Array F12. [Online] Available:
[http://sphelarpower.jp/product/pdf/datasheet_KSP-F12-xSxP-W1-X_v0912\(J\).pdf](http://sphelarpower.jp/product/pdf/datasheet_KSP-F12-xSxP-W1-X_v0912(J).pdf)
- [11] Linear Technology. LTC3588-1. [Online] Available:
<http://akizukidenshi.com/download/ds/akizuki/j35881fa.pdf>